Finite Element Modeling for Microwave Tomography

Elia A. Attardo*, Andrea Borsic*, Paul M. Meaney*, and Giuseppe Vecchi†
*Thayer School Of Engineering
Dartmouth College, 8000 Cummings Hall, Hanover, NH 03755, USA
Email: {elia.a.attardo, andrea.borsic, paul.m.meaney}@dartmouth.edu
†Politecnico di Torino
Corso Duca Degli Abruzzi 24, Turin, 10144, Italy
Email: giuseppe.vecchi@polito.it

***Abstract*—This paper presents a Finite Element Modelling for Microwave Imaging tomography based on edge basis functions. In particular a new technique is used to compute the antenna parameters. This novel procedure will provide a general method to enforce the excitation as a specific modal distribution, and to extract the voltage from the employed antenna. We show the model for the Microwave Imaging system including the antennas and we report a comparison between measured and simulated data.**

I. Introduction

Microwave Imaging (MI) has developed into a promising technique in breast cancer detection based on the different response of normal and malignant breast tissue to electromagnetic waves at microwave frequencies. Unlike radar based techniques, which have been proposed in literature for piece-wise homogeneous domains, the tomographic approach is suitable to recover the dielectric properties of an inhomogeneous medium as the breast. The reconstruction of the material properties is essentially obtained by solving an inverse problem. Generally, the result quality of an inverse problem is mostly influenced by the accuracy of the model used for forward modeling. As a consequence, having a reliable and accurate forward model is crucial especially in modelling MI system, which has a large number of antennas and complex geometry.

In the present work we focus specifically on modelling the tomographic system developed at Dartmouth College [1]. In particular we use an enhanced forward model, where we solve the 3D curl-curl Helmholtz equation using an edge Finite Element Method (FEM) via zero order Whitney forms [2]. The use of FEM techniques allows us to finely model the monopole antennas [3] used for injecting excitations and sensing. Additionally, a variational formulation is employed to extract the information related to the antenna, and to enforce a specific modal distribution, [4].

In this manuscript we firstly describe the MI system and then we show that the model can accurately predict the measured (amplitude and phase) data collected by using MI system developed at Dartmouth College.

II. Microwave imaging system

Figure 1 shows the exam table used in MI tomography for breast cancer detection at Dartmouth-Hitchcock Medical Center. The system consists of an illumination tank with antenna array, and the exam table. Both are integrated with the electronics and completely embedded in the examination table. The patient lies in prone position with her breast extending through the hole in the table. The antennas of the array are disposed on a circle around the breast under analysis. Figure 4(b) shows the illumination tank with the array in which region III represents the volume occupied by the breast, imaging domain (ID). That cylindrical region has a diameter equal to 15 cm and 20 cm of height. In addiction, in order to promote the signal-coupling and to reduce the unwanted reflections from the walls, the illumination tank is filled by a liquid-bath, which is a 80:20 percent glycerine-water solution. Figure 2 shows the relative permittivity and conductivity of this liquid as functions of frequency from 300 MHz up to 3 GHz.

Fig. 1. Examination table for MI breast cancer detection at Dartmouth-Hitchcock Medical Center.

The antenna consists of a 50 Ω coaxial cable with the outer metal conductor stripped from the termination. The length of this region is equal to 3.4 cm, [3], and it represents the radiative part of the antenna. Figure 3 shows one monopole antenna of the array.

III. Formulation

In this work we model the aforementioned MI system by FEM. In order to produce a discretized domain the infinite region exterior to the tank must be truncated. As a consequence, a boundary condition must be used. Also, since we are concentrating on experiments in microwave range, in this

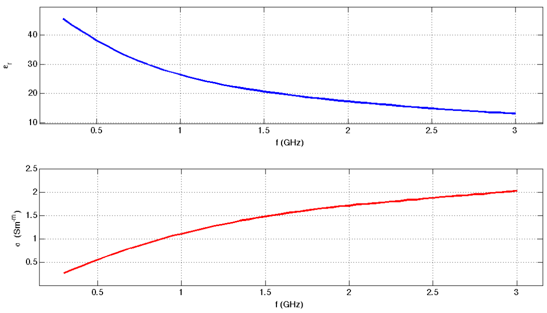

Fig. 2. Relative permittivity (blue line) and conductivity (red line) for glycerine-water 80:20 from 300MHz up to 3GHz

Fig. 3. Monopole antenna: the length of the transmitting zone is equal to 3.4 cm

work a single frequency equal to 700MHz is used, the fictitious absorbers, which have a certain thickness, have been designed to work in a wide frequency band. To this aim the most suitable absorber is a Perfectly Matched Layer (PML) [5]. According to different interpretations of PML [6] [7] we have chosen the anisotropic one [7]. Therefore, in truncating the domain boundaries is mandatory to terminate the exterior surfaces by a Perfect Electric Conductor (PEC). Thus, we can write the Maxwell's equations, source-free case, in an anisotropic medium as:

$$\nabla \times \underline{E} = -j\omega\underline{\underline{\mu}} \cdot \underline{H} \tag{1}$$

$$\nabla \times \underline{H} = j\omega\underline{\underline{\epsilon}} \cdot \underline{E} \tag{2}$$

$$\nabla \cdot (\underline{\underline{\epsilon}} \cdot \underline{E}) = 0 \tag{3}$$

$$\nabla \cdot (\underline{\underline{\mu}} \cdot \underline{H}) = 0 \tag{4}$$

where $\underline{\underline{\epsilon}}$ and $\underline{\underline{\mu}}$ are the diagonal permittivity and permeability tensors with $\underline{\underline{\epsilon}} = \epsilon_0(\underline{\underline{\epsilon_r}} - j\frac{\underline{\underline{\sigma}}}{\omega\epsilon_0})$. Also, we can readily formulate the finite element solution for the source-free case using the wave equation in tensorial fashion, namely:

$$\nabla \times [\underline{\underline{\mu}}^{-1} \cdot (\nabla \times \underline{E})] - k_0^2\underline{\underline{\epsilon}} \cdot \underline{E} = 0 \tag{5}$$

With reference to Figure 4(a) and 4(b) in region III one will perform the inverse problem trying to reconstruct the material

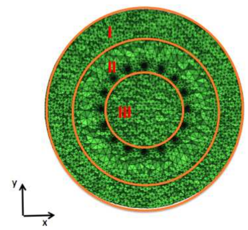

(a) Meshed domain, cross section along z axis: region I is the PML; region II represents the external domain of ID; region III is the ID

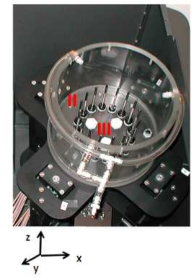

(b) Tank with 16 monopole antennas: external domain (region II) and imaging domain (region III)

Fig. 4. MI System

properties of the breast under investigation. It is worth noting that with this work we do not address the inverse problem but we rather describe the forward one. Therefore, having an accurate solution of Maxwell's equation inside the ID is a mandatory starting point for the inversion procedure.

As mentioned before, we use edge-based FEM with vector basis functions defined on tetrahedral elements [2]. Figure 4(a) illustrates the built mesh obtained by using Netgen mesh generator [8]. Recalling equation (5) it is possible associate a homogeneous Boundary-Value problem (BVP) by enforcing the tangential component of the electric field equal to zero on PEC surface, $\hat{n} \times \underline{E} = 0$. Consequently, the associated anisotropic variational formulation is expressed as:

$$\mathcal{F}(\underline{E}) = \frac{1}{2}\iiint_V [(\nabla\times\underline{E}^*)\cdot\frac{1}{\underline{\underline{\mu}}_r}\cdot(\nabla\times\underline{E}) - k_0^2\underline{E}^*\cdot\underline{\underline{\epsilon}}\cdot\underline{E}]dV \tag{6}$$

where $\underline{E}^*$ is the complex conjugate of the electric field $\underline{E}$. As usual the region I in Figure 4(a) represents the PML with the exterior surfaces set as PEC. The attenuation rule for tetrahedral elements inside the PML region was chosen according to [9].

Moreover, choosing the edge basis functions $\underline{W}$ we apply the Galerkin's test procedure to (6) in order to produce a discretized version of the functional:

$$\begin{aligned}[M]_{ij} = &\iiint_V (\nabla \times \underline{W}_i)\frac{1}{\underline{\underline{\mu}}} \cdot (\nabla \times \underline{W}_j)dV + \\ &-k_0^2 \iiint_V \underline{W}_i \cdot [\underline{\underline{\epsilon_r}}] \cdot \underline{W}_j dV + \\ &+j\omega\mu_0 \iiint_V \underline{W}_i[\underline{\underline{\sigma}}]\underline{W}_j dV\end{aligned} \tag{7}$$

where $[M]_{ij}$ is a generic element of the FEM matrix, $\underline{\underline{\epsilon_r}}$ and $\underline{\underline{\sigma}}$ the relative permittivity and conductivity tensors respectively.

IV. Antenna parameters

In this section we describe the relation between the forcing term and the characteristic antenna parameters, (i.e.: internal

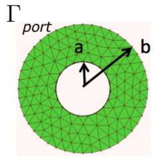

Fig. 5. Coaxial port surface: a and b are the inner and outer conductors' radii respectively.

impedance). According to [4] if a guiding structure (e.g.: coaxial cable) is used as feeding point the impedance is associated with the mode of the port itself. In our case the monopole antenna is fed by a coaxial line and we firstly enforce a field boundary condition representing the excitation on that port surface. Secondly, we will obtain the desired voltage once we have computed the solution of the FEM system.

A. Enforcing field boundary conditions

We provide the excitations of each of the monopoles in Figure 4(b) by enforcing a Dirichlet boundary condition for the electric field on the coaxial port surface Γ_{port}. The field boundary condition will be enforced in terms of modal field. According to Figure 5 we can write the enforced boundary condition for the electric field as:

$$\widehat{n} \times \underline{E} = \underline{E}_0 = V_p \underline{e^\dagger} \tag{8}$$

where $\hat{n}$ the is normal to the coaxial port surface, V_p the voltage between the b and a, and $\underline{e}^\dagger$ is the transverse-electromagnetic (TEM) modal eigenfunction of the feeding coaxial cable [10]:

$$\underline{e}^\dagger = \widehat{\rho} \frac{1}{\sqrt{2\pi\rho \cdot ln(b/a)}} \tag{9}$$

being ρ a local radial coordinate over Γ_{port}.

B. Extracting internal impedance

In this section we describe the procedure used to compute the internal impedance for a receiver antenna. In doing that we need to use two different antennas: one as transmitter and the other one as receiver. Using that configuration allows us to characterize the antenna in receiving mode. The distance between the two antennas is greater than $2D^2/\lambda_g$ where λ_g is the wavelength with respect to glycerine bath permittivity and D is the largest dimension of the monopole. We first compute the primary field, which is a function of the defined voltage V_p, using only the transmitter antenna and then we insert the receiver one. In addition, the concept of impedance is used once we have obtained the solution of the FEM system. As matter of fact, starting from that solution, it is possible to calculate the magnetic field, and it is possible to enforce the impedance relationship as:

$$\underline{H}(\underline{r}) = \frac{1}{Z} V_p (\hat{n} \times \underline{e}\dagger) \frac{ln(b/a)}{2\pi} \tag{10}$$

Yet, we compute (10) on Γ_{port}, obtaining the internal impedance, $Z = Z_{INT}$, jointly with the current expressed as:

$$I = \oint_{\partial\Gamma_{port}} \underline{H} \cdot dl \tag{11}$$

As a consequence, the voltage associated with *i*th antenna is written as:

$$V_i = Z_{INT} \cdot I \tag{12}$$

V. Results

In this section we validate the procedures outlined in IV by making a comparison with measured data. For the time being, we consider only the tank with the coupling liquid without any object inside. Further, those procedures are completely independent to the experiment set-up and one can use them in a complex environment without any modifications. Setting the frequency equal to $f = 700$ MHz, and considering all 16 antennas, as is shown in Figure 4(b), we report the simulated and measured voltage for each transmitter. With regards to Figure 6 the notation proposed in [11] is used. In Figure 6(a) and 6(b) it is possible notice a good agreement between the simulated and measured voltage amplitude for all transmitter antennas. However, as one can observe in Figure 6(a), oscillations in the amplitude for the measured voltage related to the eighth relative receiver, which is the opposite receiver for one transmitter antenna, could appear due to the amplifier's noise floor proximity and due to a low SNR. For the sake of simplicity, we show only the phase for one transmitter, Figure 6(c).

VI. Conclusions

In this work we have presented a FEM modelling for MI tomography. In particular, a new technique able to compute the voltage associated with a receiver was shown. The aforementioned technique allows us to deal with the complex geometry of the imaging system without using any approximations in modelling the antennas. Those procedures were tested in a simple environment in which only the tank and glycerine bath were present. Naturally, it could be possible to extend all the procedures herein presented to a more general case without jeopardise the result quality of the technique. For instance objects inside the imaging domain would be considered.

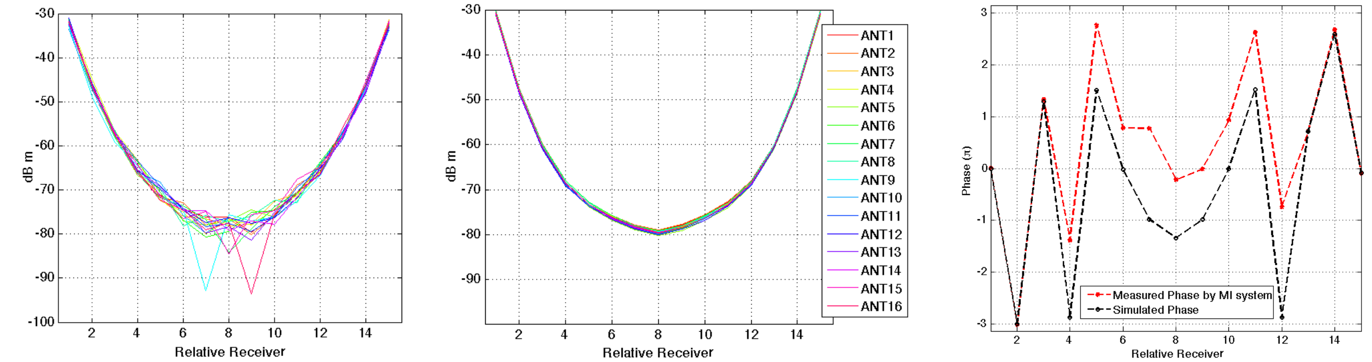

(a) Measured amplitude voltage by MI system for all 16 antennas

(b) Simulated amplitude voltage for all 16 antennas

(c) Measured (red line) and simulated (black line) phase for one transmitter

Fig. 6. Comparison between measured and simulated voltage (amplitude and phase)

REFERENCES

[1] K.D. Paulsen, P.M. Meaney, L.C. Gilman *Alternative Breast Imaging*, Springer-Verlang, 2005

[2] J.C. Nedelec, *Mixed Finite Elements in* R^3, Numerische Mathematik, 35,Periodical 28 page(s) (315 - 342)

[3] C. J. Fox, P. M. Meaney, F. Shubitidze, L. Potwin, and K. D. Paulsen *Characterization of an Implicitly Resistively-Loaded Monopole Antenna in Lossy Liquid Media* , Int. J. of Ant. and Prop. Volume 2008

[4] D. Milanesio, O. Meneghini, V. Lancellotti, R. Maggiora and G. Vecchi *A multi-cavity approach for enhanced efficiency in TOPICA RF antenna code*, Nuclear Fusion, 2009

[5] J.P. Berenger, *Perfectly Matched Layer for Computational Electromagnetics*, Morgan and Claypool, 1994

[6] W.C. Chew, *A 3D perfectly matched medium from modified Maxwells equation with stretched coordinate*, Micr.Opt.Tech.Let.,1994

[7] Z.S. Sacks, R.Lee, J.-F. Lee, *A perfectly matched anisotropic for use as an absorbing boundary conditions*, EEE Trans.Ant. Prop.,1995

[8] http://www.hpfem.jku.at/netgen/

[9] A. Greenwood, J.M. Jin, *A Novel Efficient Algorithm for Scattering from a Complex BOR Using Mixed Finite Elements and Cylindrical PML*, IEEE Trans.Ant. Prop. 1999

[10] N. Marcuvitz, *Waveguide Handbook*, 1951, New York: McGraw-Hill

[11] P. M. Meaney, K. D. Paulsen, B. W. Pogue,and M. I. Miga, *Microwave Image Reconstruction Utilizing Log-Magnitude and Unwrapped Phase to Improve High-Contrast Object Recovery*, IEEE Trans.on Med. Im., vol. 20, NO. 2, 2001